Comparing two atlas-based automatic segmentation methods for subthalamic nucleus deep brain stimulation

Y. Xiao[1], L. Bailey[1], M. Mallar Chakravarty[2], S. Beriault[1], A. F. Sadikot[3], G. Bruce Pike[1], and D. Louis Colins[1]

[1]*McConnell Brain Imaging Centre, Montréal Neurological Institute, McGill University, Montréal, Québec, Canada,* [2]*Kimel Family Translational Imaging-Genetic Laboratory, Research Imaging Centre, Centre for Addiction, Toronto, Canada,* [3]*Division of Neurosurgery, McGill University, Montréal, Canada*

Introduction: Deep brain stimulation (DBS) of the subthalamic nucleus (STN) is an effective treatment for Parkinson's disease (PD). Since the STN has a small size and is divided into three functional regions (motor, associative and limbic), it is important to localize the stimulation target to avoid undesirable side-effects and achieve the best therapeutic benefits for the patients. Previously, automatic segmentation of the basal ganglia nuclei was achieved through non-rigid histological atlas warping [1,2]. In this abstract, this method is compared with a novel *in vivo* T2 data derived atlas warping strategy for their segmentation performance on the STN, red nucleus (RN), and substantia nigra (SN). The manual segmentations of these three nuclei from the susceptibility-based 3T MR images were used as a silver standard for evaluation.

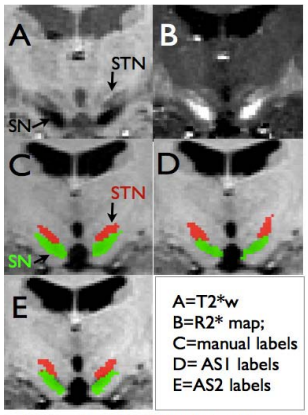

Figure 1. SN and STN of a 41 yo healthy female subject

Methods: After providing informed consent, 2 healthy subjects (male, 24yr & female, 41yr) and 4 PD patients (1 female, 3 male, age = 56±6yr) volunteered for the study. Each subject was scanned on a 3T MRI scanner (Siemens Trio, Erlangen, Germany) with a 10 echo 3D FLASH MRI protocol: TE={1.6, 4.1, 6.6, 9.1, 13.0, 16.0, 18.5, 21.0, 23.5, 26.0}ms, TR=30ms, flip-angle=23°, BW=±450 Hz/pix, matrix=256x256, 176 sagittal slices, resolution= 0.95x0.95x0.95mm^3, 6/8 partial Fourier in the phase and slice encoding directions, and GRAPPA=2. From the MRI data acquired, three image contrasts (T1w image, T2*w image, and R2* map) were generated. The T1w image was produced by averaging the magnitude images of the first four echoes. The T2*w image was generated by averaging the magnitude of the last five echoes. The R2* map was derived by fitting all magnitude data to an exponential curve. With ITK-SNAP (www.itkSNAP.org), we obtained the silver standard by manually segmenting the STN, SN, and RN on each subject in 3D using a consensus of their T2*w images and R2* maps. The first atlas-based segmentation method (referred to as "**AS1**") was described in [2] where histological data, structural outlines and a T1w single subject average MRI known as Colin27 [3], are non-linearly warped to a patient's T1w volume to achieve segmentation. In the second method ("**AS2**"), the atlas structures are obtained by manually painting the STN, SN, and RN on the Colin12 T2w image, a single subject average of 12 T2w volumes [3], co-registered with the Colin27 T1w image. Segmentation in **AS2** is achieved by warping the T2w-defined labels using the transforms estimated in **AS1**. **AS1** and **AS2** segmentations are compared to the silver standard manual labels with three metrics: 1) the overlap metric **kappa=2*a/(b+c)**, where **a** is the mutual volume of two segmentations, and **b** and **c** are volumes belong to each segmentation; 2) the Euclidean distance (**COM_Euclid**) between the centre of mass (COM) of the deformed atlas labels and manual segmentation; and 3) the x-, y-, and z-coordinate COM differences (**COM{x,y,z}=COM$_{atlas}$ – COM$_{manual}$**) after transforming them into Talairach space.

Results: Three metrics are presented in Table 1 with the mean values and standard deviations of all 6 subjects .

	Left RN			Right RN			Left SN			Right SN			Left STN			Right STN		
Kappa	0.56±0.08 / 0.70±0.06			0.50±0.11 / 0.72±0.08			0.58±0.04 / 0.54±0.04			0.61±0.01 / 0.57±0.09			0.55±0.08 / 0.55±0.07			0.41±0.17 / 0.53±0.07		
COM_Euclid(mm)	1.72±0.40 / 1.24±0.42			2.35±0.56/ 1.06±0.54			2.08±0.67/2.56±0.30			1.65±0.73/ 2.07±0.69			1.64±0.63/1.35±0.42			2.66±0.96/1.52±0.63		
	x	y	z	x	y	z	x	y	z	x	y	z	x	y	z	x	y	z
COM{x,y,z}(mm)	-0.28±0.54	-1.50±0.24	-0.89±0.37	1.68±0.73	-0.86±0.37	-1.52±0.32	1.58±0.49	1.49±0.48	0.44±0.43	-1.00±0.44	1.29±0.62	0.33±0.38	-1.29±0.53	0.09±0.99	-0.62±0.52	1.91±1.20	-0.39±0.90	-1.60±0.47
	0.32±0.53	0.97±0.44	0.68±0.35	-0.23±0.77	0.60±0.51	0.58±0.32	0.38±0.55	-2.44±0.54	0.72±0.37	0.11±0.36	-2.00±0.75	0.70±0.20	0.26±0.64	0.79±1.06	0.52±0.66	0.35±1.07	0.34±0.98	0.60±0.56

Table 1. The mean value and standard deviation for the three metrics (**black**=**AS1**, **blue**=**AS2**). Please note that for COM{x,y,z}, x-coordinate = left-right direction, y-coordinate=anterior-posterior direction, and z-coordinate=superior-inferior direction.

Conclusion: Overall, there is a coarse correspondence between **AS1** and **AS2** segmentations and the manual segmentation, but the performance of each segmentation method differ for various structures. First, the kappa metric shows that **AS2** performs significantly better than **AS1** for the RN ($p<0.02$), and on average better for the right STN. Their performances does not differ significantly for other structures. Second, the COM Euclidean distances of **AS1** segmentations and manual segmentations are on average larger than that for **AS2** on the RN and STN, significantly so for the right RN and STN ($p<0.05$). As the "key" structure of DBS, **AS2** offers a comparable or better segmentation for the STN bilaterally. Through the analysis of the x-, y-, and z-coordinate COMs positions, the **AS1** segmentation was more lateral and superior than the silver standard STN ($p<0.05$), more medial and posterior for the SN ($p<0.01$), and more anterior and superior for the RN ($p<0.01$); On the other hand, **AS2** segmentation was more posterior and inferior for the RN ($p<0.01$), and more anterior and inferior for the SN ($p<0.01$). In summary, the Colin12 T2w-image-defined atlas was more successful in the group we studied.

Discussion: Notably, the segmentation of the right STN for **AS1** method was significantly worse than that of the left STN in terms of kappa and COM Euclidean distances ($p<0.05$), but no significant difference in bilateral segmentation of the STN was found in **AS2**. This could be explained by the fact that the histological atlas (**AS1**) was defined symmetrically while there was no such assumption for **AS2**. In our subjects, the averaged left STN size was larger than the right, and Colin27 left STN is also larger than the right as shown in the T2w image. **AS2**'s better performance on the RN, and its worse mean COM Euclidean distances on the SN suggest that the T1w-T1w inter-subject or pesudo-MRI-to-subject registration may not fully account for the variability in these nuclei [4] that are almost invisible on the T1w images. In **AS1**, the histologically defined STN has a relatively small size (left-right-averaged: 170 mm^3), and for **AS2**, the *in vivo* data derived atlas has a relatively smaller SN (left-right-averaged: 484 mm^3) than the averages of the studied population (left-right-averaged RN: 224 mm^3; left-right-averaged SN:527mm^3). As a result, without proper constraints, these biases from the single subject defined atlas could not be fully neutralized during the mapping to different subjects, resulting in sub-optimal segmentations. Moreover, the neuron loss in PD subjects may further enhance this atlas-inherent bias since most of the currently used atlases were obtained from healthy subjects. As a result, incorporating image contrasts that can visualize these structures should be instrumental to the more accurate automatic segmentation of the SN, RN, and more particularly the STN.

Reference: 1. Chakravarty *et al*. NeuroImage 30 (2006) 359 –376; **2**. Chakravarty *et al*. Med. Image Anal. 12 (2008) 713–726; **3.** Holms *et al*. J Comput Assist Tomogr. 1998 Mar-Apr; 22(2): 324-33; **4.**. Daniluk *et al*. Acta Neurochir (2010) 152:201–210.